CHEMISTRY OF MATERIALS
Article

Chem. Mater. **2010,** *22,* 3015–3020 3015
DOI:10.1021/cm1004714

Nanosized Tetragonal $BaTiO_3$ Powders Synthesized by a New Peroxo-Precursor Decomposition Method

Isao Tsuyumoto,* Mitsuru Kobayashi, Tomohide Are, and Naoya Yamazaki

Department of Applied Chemistry, College of Bioscience and Chemistry, Kanazawa Institute of Technology 7-1 Ohgigaoka, Nonoichi, Ishikawa 921-8501, Japan

Received February 14, 2010. Revised Manuscript Received March 8, 2010

A new peroxo-precursor decomposition method is developed for synthesis of $BaTiO_3$. Peroxo-polytitanic acid solution is prepared by reaction between metallic titanium powder and H_2O_2 aq, and the amorphous peroxo-precursor is prepared by mixing the peroxo-polytitanic acid with $Ba(OH)_2$ aq. The reaction time between the metallic titanium powder and H_2O_2 aq is shortened from 72 to 6 h by increasing the concentration of H_2O_2 aq from 30 to 70 wt %. $BaTiO_3$ with crystallite size of 14.7−419.7 nm and tetragonality c/a of 1.0037−1.0090 is obtained by heating the precursor for 1 h at 600−1150 °C in air. $BaTiO_3$ obtained at 650 °C shows a uniform size distribution in the field-emission scanning electron microscope (FE-SEM) image around 30 nm, and the dielectric constant of 360.

Introduction

Barium titanate ($BaTiO_3$) is an important electroceramic material used for multilayer ceramic capacitors (MLCC), positive temperature coefficient (PTC) thermistors, and electro-optic devices, because it has high dielectric permittivity and ferroelectric properties. $BaTiO_3$ powders with small grain size and high dielectric permittivity are desirable for the applications to the MLCC because the downsizing of the MLCC is achieved by using thin ceramic layers with high dielectric permittivity. The conventional solid state reaction between $BaCO_3$ and TiO_2 around 1250 °C has been mainly employed to synthesize $BaTiO_3$ since the discovery of its ferroelectricity in the 1940s. The solid state reaction between $BaCO_3$ and TiO_2 has been reported to occur in three basic stages: first, formation of a surface layer of $BaTiO_3$ on the outer surface regions of TiO_2 by the diffusion of Ba^{2+} ions into TiO_2; second, formation of Ba_2TiO_4 by further diffusion of Ba^{2+} ions and reaction with the prior-formed $BaTiO_3$; and finally, the reaction between Ba_2TiO_4 and remaining TiO_2 to form $BaTiO_3$.[1−4] Such complex reaction mechanism necessitates repeated calcination and regrinding in long periods, and the long high temperature process brings about irregular crystal growth and uncontrolled particle morphology. Novel processes that allow the preparation of homegeneous $BaTiO_3$ at relatively low temperatures are highly desirable to obtain fine particles for the MLCC applications.

In recent years, soft-chemical processes such as the hydrothermal method,[5−21] the sol−gel method,[22−28] and the precursor decomposition method[29−32] have been intensively investigated to prepare $BaTiO_3$, and

*To whom correspondence should be addressed. E-mail: tsuyu@neptune.kanazawa-it.ac.jp.

(1) Mutin, J. C.; Niepce, J. C. *J. Mat. Sci. Lett.* **1984**, *3*, 591–592.
(2) Beauger, A.; Mutin, J. C.; Niepce, J. C. *J. Mat. Sci.* **1984**, *19*, 195–201.
(3) Beauger, A.; Mutin, J. C.; Niepce, J. C. *J. Mat. Sci.* **1983**, *18*, 3543–3550.
(4) Beauger, A.; Mutin, J. C.; Niepce, J. C. *J. Mat. Sci.* **1983**, *18*, 3041–3046.
(5) Kubo, T.; Hogiri, M.; Kagata, H.; Nakahira, A. *J. Am. Ceram. Soc.* **2009**, *92*, S172–S176.
(6) Kwon, S. G.; Choi, K.; Kim, B. *Mater. Lett.* **2005**, *60*, 979–982.
(7) Kwon, S. G.; Park, B. H.; Choi, K.; Choi, E. S.; Nam, S.; Kim, J. W.; Kim, J. H. *J. Eur. Ceram. Soc.* **2006**, *26*, 1401–1404.
(8) Sun, W.; Li, C.; Li, J.; Liu, W. *Mater. Chem. Phys.* **2006**, *97*, 481–487.
(9) Hirasawa, M.; Kajiyoshi, K.; Yanagisawa, K. *J. Am. Ceram. Soc.* **2005**, *88*, 1415–1420.
(10) Kim, Y.; Jung, J. K.; Ryu, K. *Mater. Res. Bull.* **2004**, *39*, 1045–1053.
(11) Lu, S. W.; Lee, B. I.; Wang, Z. L.; Samuels, W. D. *J. Cryst. Growth* **2000**, *219*, 269–276.
(12) Clark, I. J.; Takeuchi, T.; Ohtori, N.; Sinclair, D. C. *J. Mater. Chem.* **1999**, *9*, 83–91.
(13) Bocquet, J. F.; Chhor, K.; Pommier, C. *Mater. Chem. Phys.* **1999**, *57*, 273–280.
(14) Ma, Y.; Vileno, E.; Suib, S. L.; Dutta, P. K. *Chem. Mater.* **1997**, *9*, 3023–3031.
(15) Shi, E.; Xia, C.; Zhong, W.; Wand, B.; Feng, C. *J. Am. Ceram. Soc.* **1997**, *80*, 1567–1572.
(16) Eckert, J. O., Jr.; Hung-Houston, C. C.; Gersten, B. L.; Lencka, M. M.; Riman, R. E. *J. Am. Ceram. Soc.* **1996**, *79*, 2929–2939.
(17) Asiaie, R.; Zhu, W.; Akbar, S. A.; Dutta, P. K. *Chem. Mater.* **1996**, *8*, 226–234.
(18) Slamovich, E. B.; Aksay, I. A. *J. Am. Ceram. Soc.* **1996**, *79*, 239–247.
(19) Noma, T.; Wada, S.; Yano, M.; Suzuki, T. *J. Appl. Phys.* **1996**, *80*, 5223–5233.
(20) Begg, B. D.; Vance, E. R.; Nowotny, J. *J. Am. Ceram. Soc.* **1994**, *77*, 3186–3192.
(21) Christensen, A. N. *Acta Chem. Scand.* **1970**, *24*, 2447–2452.
(22) Devaraju, N. G.; Lee, B. I.; Wang, X.; Viviani, M.; Nanni, P. *J. Mat. Sci.* **2006**, *41*, 3335–3340.
(23) Takeuchi, T.; Tabuchi, M.; Ado, K.; Honjo, K.; Nakamura, O.; Kageyama, H.; Suyama, Y.; Ohtori, N.; Nagasawa, M. *J. Mat. Sci.* **1997**, *32*, 4053–4060.
(24) Shimooka, H.; Kuwabara, M. *J. Am. Ceram. Soc.* **1996**, *79*, 2983–2985.
(25) Frey, M. H.; Payne, D. A. *Phys. Rev. B* **1996**, *54*, 3158–3168.
(26) Frey, M. H.; Payne, D. A. *Chem. Mater.* **1995**, *7*, 123–129.
(27) Schlag, S.; Eicke, H. F. *Solid State Commun.* **1994**, *91*, 883–887.
(28) Pfaff, G. *J. Mater. Chem.* **1992**, *2*, 591–594.
(29) Wada, S.; Yasuno, H.; Hoshina, T.; Nam, S. M.; Kakemoto, H.; Tsurumi, T. *Jpn. J. Appl. Phys.* **2003**, *42*, 6188–6195.

Published on Web 03/25/2010

the preparation of nanosized $BaTiO_3$ powders through such processes have been reported by many researchers.[5,10,11,22,29,30] Such processes have advantages over the conventional solid state reactions to prepare homogeneous and fine powders because nucleation in aqueous solution or amorphous solid matrix, and subsequent crystalline growth by precipitation from solution or thermal decompostion of solid phase, proceed at lower temperatures. To ensure the quality of the products, it is essential to mix raw materials equally at microscopic scale, and the fine raw materials are usually dispersed in a liquid to mix them equally in the conventional solid state reaction process. In the soft-chemical processes, barium and titanium are mixed equally at nanometer scale, and they are appropriate for the preparation of ordinary particles, as well as of nanosized particles. In general, the ferroelectric $BaTiO_3$ belongs to the tetragonal perovskite crystal structure, and its ferroelectricity vanishes because of the phase transition to the cubic phase at high temperature, that is, the tetragonality enormously contributes to its ferroelectricity. However, superfine $BaTiO_3$ directly precipitated in the hydrothermal processes have been reported to show lower tetragonality (expressed by the c/a ratio of lattice parameters). A number of studies have been made to attain high tetragonality in hydrothermal synthesis.[6−8,13,14] A two-step thermal decomposition method of barium titanyl oxalate has been proposed to prepare nanosized $BaTiO_3$.[29,30] Thermal decomposition processes using precursors containing the elements other than Ba, Ti, and O may cause impurities in the product, and thus precursors containing only Ba, Ti, and O are highly desirable for the synthesis.

We have developed a new technique for preparing metal oxides from peroxo-poly metallic acid obtained by direct reaction between metallic powder and hydrogen peroxide solution. For example, peroxo-polytungstic acid is obtained by vigorous reaction between metallic tungsten powder and hydrogen peroxide solution, and an amorphous precursor is precipitated by mixing an alkali solution with the peroxo-polytungstic acid.[33−35] Heating the precursor at 500−700 °C yields alkali tungstates or tungsten bronzes. Similarly, molybdenum, niobium, vanadium, and titanium powders react with hydrogen peroxide, and yield the corresponding peroxo-polymetallic acids.[36−39] However, the reaction of the titanium powder with the hydrogen peroxide was markedly slow compared to the other metals, for example, 11 g of tungsten powder dissolves into 70 mL of 20 wt % H_2O_2 aq in 30 min, whereas it takes a few days for 0.1 g of titanium powder to dissolve into 100 mL of 30 wt % H_2O_2 aq. To accelerate the reaction, it has been proposed to start from alkoxides or titanium tetrachloride instead of metallic titanium powder and to use the additives such as ammonia.[40−44] Some researchers have reported the preparation of the titanium dioxide thin films through such peroxo routes.[45,46]

In this study, we developed a new synthetic route of $BaTiO_3$ fine powders from peroxo-polytitanic acid obtained by mixing the titanium powder and the hydrogen peroxide. We considered that starting from titanium powder without any additives is appropriate to prepare pure products and successfully accelerated the reaction by using more concentrated H_2O_2 solutions (40−70 wt %). We present here the synthetic details of the $BaTiO_3$ and its characterizations using Rietveld refinement of X-ray diffraction (XRD), field-emission scanning electron microscope (FE-SEM) observation, and dielectric constant measurement.

Experimental Section

Synthesis. Metallic Ti powder (0.12 g, 95%, 45 μm particle size, as received from Wako Pure Chemical Industries, Ltd., Osaka, Japan) was dissolved in 100 mL of 30 wt % H_2O_2 solution (Wako Pure Chemical Industries, Ltd., Osaka, Japan) at 20 °C with stirring. A yellow transparent solution of peroxo-polytitanic acid (denoted as Ti-IPA where IPA stands for isopolyacid) was obtained in 72 h. After removing insolubles by filtration, we used the solution for the synthesis. By mixing the Ti-IPA solution with 100 mL of 28 mmol/L $Ba(OH)_2$ aqueous solution, we obtained an amorphous barium peroxo-polytitanate as a white yellow precipitate. After storage for 24 h. at 20 °C, the precipitate was filtered, rinsed with water and dried at 115 °C. By heating the amorphous barium peroxo-polytitanate in air at 600, 650, 1000, and 1150 °C, we obtained polycrystalline barium titanates.

To accelerate the reaction between H_2O_2 and Ti, the H_2O_2 solution was concentrated up to 70 wt % by distillation under diminished pressure using a rotary evaporator at 37 °C. The concentrated H_2O_2 solution contained almost the same molar amount of H_2O_2 as before the concentration, for example, 38 mL of 70 wt % H_2O_2 and 46 mL of 60 wt % H_2O_2 were prepared from 100 mL of 30 wt % H_2O_2. Polycrystalline barium titanates were prepared by the same procedure as stated above.

Characterization. The ultraviolet−visible (UV−vis) absorption spectra of the Ti-IPA solutions were taken using a spectrophotometer (V570, JASCO, Tokyo, Japan), and the time-course of the absorbance at 400 nm was measured to monitor the reaction rate between Ti and H_2O_2 aq. The thermal behavior of the amorphous precursor was investigated by thermogravimetry (TG) and differential thermal analysis (DTA; DTG-50, Shimadzu, Kyoto, Japan)

(30) Wada, S.; Narahara, M.; Hoshina, T.; Kakemoto, H.; Tsurumi, T. *J. Mat. Sci.* **2003**, *38*, 2655–2660.
(31) Cho, W. S. *J. Phys. Chem. Solid* **1998**, *59*, 659–666.
(32) Hsiang, H.; Yen, F. *J. Am. Ceram. Soc.* **1996**, *79*, 1053–1060.
(33) Tsuyumoto, I.; Kudo, T. *Mater. Res. Bull.* **1996**, *31*, 17–28.
(34) Tsuyumoto, I.; Kudo, T. *Sens. Actuators, B* **1996**, *30*, 95–99.
(35) Tsuyumoto, T.; Kishimoto, A.; Kudo, T. *Solid State Ionics* **1993**, *59*, 211–216.
(36) Yagi, Y.; Hibino, M.; Kudo, T. *J. Electrochem. Soc.* **1997**, *144*, 4208–4212.
(37) Kudo, T.; Sasaki, Y.; Hashimoto, M.; Matsumoto, K. *Inorg. Chim. Acta* **1988**, *145*, 205–209.
(38) Kudo, T.; Okamoto, H.; Matsumoto, K.; Sasaki, Y. *Inorg. Chim. Acta* **1986**, *111*, L27–L28.
(39) Kudo, T. *Nature* **1984**, *312*, 537–538.
(40) Tsuyumoto, I.; Nawa, K. *J. Mat. Sci.* **2008**, *43*, 985–988.
(41) Tsuyumoto, I.; Nawa, K. *Solid State Ionics* **2008**, *179*, 1227–29.
(42) Ichinose, H.; Taira, M.; Furuta, S.; Katsuki, H. *J. Am. Ceram. Soc.* **2003**, *86*, 1605–1608.
(43) Tada, M.; Yamashita, Y.; Petrykin, V.; Osada, M.; Yoshida, K.; Kakihana, M. *Chem. Mater.* **2002**, *14*, 2845–2846.
(44) Ichinose, H.; Terasaki, M.; Katsuki, H. *J. Ceram. Soc. Jpn.* **1996**, *104*, 715–718.
(45) Wang, Z.; Hu, X. *Thin Solid Films* **1999**, *352*, 62–65.
(46) Natarajan, C.; Fukunaga, N.; Nogami, G. *Thin Solid Films* **1998**, *322*, 6–8.

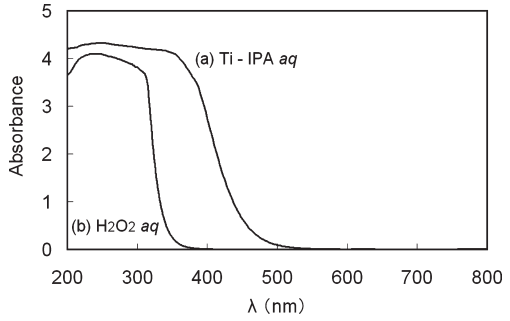

Figure 1. UV−Vis spectra of (a) Ti-IPA solution containing 0.045 mol/L of Ti and (b) 30 wt % H_2O_2 solution.

at a heating rate of 20 °C/min. The morphologies of the barium titanates obtained at 650, 1000, and 1150 °C were observed by FE-SEM (SU-70, Hitachi, Tokyo, Japan) with an accelerating voltage of 0.7 kV. The XRD patterns of the products were measured with a diffractometer (XD-D1, Shimadzu, Kyoto, Japan) using graphite - monochromatized Cu $K\alpha$ radiation (λ = 0.15406 nm) at 30 kV and 30 mA. The X-ray profiles were collected between 2° and 120° of 2θ angles with a step interval of 0.02° and a count time of 1 s/step. The crystalline parameters of the obtained $BaTiO_3$ were refined by the Rietveld method using the RIETAN-2000 program.[47] The crystallite sizes of $BaTiO_3$ were determined by

$$p = 180K\lambda/\pi X \quad (1)$$

where p is the crystallite size, K is the Scherrer constant (0.9), λ is the wavelength of X-ray, and X is a peak profile parameter, the Lorentzian Scherrer broadening obtained in the Rietveld refinement. The Ba/Ti molar ratios of the specimens were determined by X-ray fluorescence spectrometry (XRF-1700, Shimadzu, Kyoto, Japan) using the fundamental parameter (FP) method. Dielectric constant measurement using the complex impedance plot (50 Hz−5 MHz) was performed on the pellet (5 mm × 8 mm × 0.54 mm) of the obtained $BaTiO_3$ fabricated by monoaxial pressing at 200 MPa. The capacitance C of the pellet was calculated from the relationship,

$$2\pi fRC = 1$$

where f is the frequency at the top of semicircle and R is the diameter of the semicircle.

Results and Discussion

Preparation and Properties of Ti-IPA Solution. The UV−vis spectrum of the Ti-IPA solution (0.045 mol/L as to Ti) is shown in Figure1 along with that of 30 wt % H_2O_2 solution. The Ti-IPA solution showed a wide and strong absorption band extending from the UV to the Vis region and decaying at around 500 nm, whereas the H_2O_2 solution showed a strong absorption band only in the UV region. The molar extinction coefficient (ε) of Ti-IPA solution at 400 nm was estimated as 6.11×10^4 cm^2 mol^{-1}. The absorption in the range of 320−500 nm is considered to be due to electronic transitions in the titanium complex ion with a peroxo group as a ligand. We observed the absorbance at 400 nm to monitor the concentration of the Ti-IPA during the reaction between Ti and H_2O_2 because H_2O_2 showed no absorption at 400 nm.

(47) Izumi, F.; Ikeda, T. *Mater. Sci. Forum* **2000**, *321−324*, 198–205.

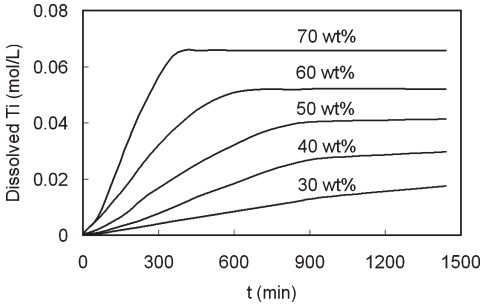

Figure 2. Time courses of Ti-IPA concentration estimated from the absorbance at 400 nm after mixing Ti powders with H_2O_2 solutions (30−70 wt %).

Figure 2 shows the time-courses of Ti-IPA concentration after mixing Ti powders and H_2O_2 solutions (30−70 wt %). The reaction rate was remarkably increased with increasing the concentration of H_2O_2 solution. The reaction was completed in 6 h when 70 wt % H_2O_2 was used, while a few days were needed to complete the reaction with 30 wt % H_2O_2. The reaction rate curves in Figure 2 were well fitted with a third reaction, whose rate equation is expressed by

$$\mathrm{d[Ti\text{-}IPA]}/\mathrm{d}t = km_{\mathrm{Ti}}[\mathrm{H_2O_2}]^2 \quad (2)$$

where m_{Ti} is a molar amount of Ti dispersed in 1 L of the solution. The rate coefficient k was estimated as 1.4×10^{-7} L^2 mol^{-2} s^{-1}. The reaction between H_2O_2 and Ti is simply expressed by

$$\mathrm{Ti} + 2\mathrm{H_2O_2} \rightarrow \mathrm{Ti\text{-}IPA} \quad (3)$$

This may suggest that the Ti-IPA ion contains two peroxo groups or H_2O_2 molecules as ligands.

The reaction rate of this peroxo-route was substantially improved by using the concentrated H_2O_2 solutions. It is also expected that the peroxo-route will be applied to industrial manufacture of photocatalyst thin films because aqueous solutions containing titanium is especially useful for preparing TiO_2 thin films. Additionally, heating the mixture of Ti and H_2O_2 above 50 °C makes the solution turbid because of decomposition of the titanium complex, and thus the reaction cannot be accelerated by heating.

The Ti-IPA solution formed a yellow gelatinous precipitate by drying at room temperature. In TG measurement, the gelatinous precipitate showed weight loss by 95.8% in the range of room temperature to 210 °C and formed a yellow amorphous powder. The amorphous powder crystallized into the anatase TiO_2 around 330 °C and into the rutile TiO_2 around 700 °C.

Preparation of $BaTiO_3$ and Its Characterizations. Figure 3 shows the TG and DTA curves for the amorphous barium peroxo-polytitanate precipitated by mixing the Ti-IPA solution with $Ba(OH)_2$ aqueous solution (see Experimental Section). A broad endothermic peak accompanied by gradual weight decrease was observed from room temperature to around 160 °C because of desorption of hydrated water. An exothermic peak accompanied by a steep weight decrease around 594 °C indicates that the amorphous salt

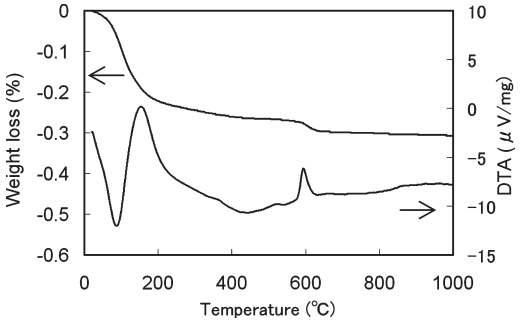

Figure 3. TG and DTA curves of the amorphous precursor, barium peroxo-polytitanate, at heating rate 20 °C/min in air.

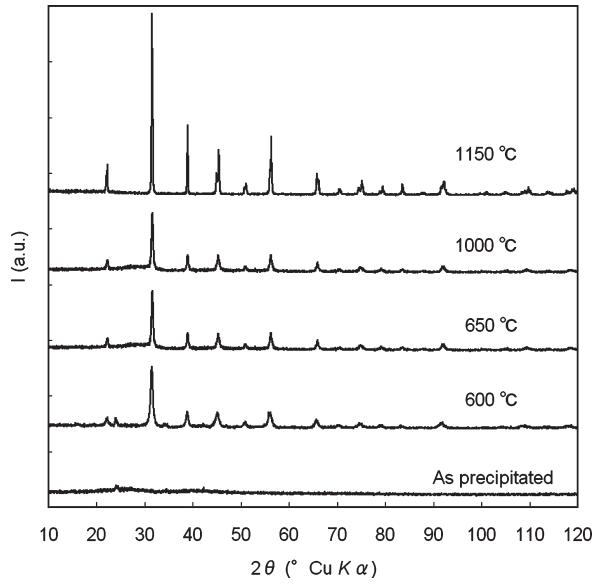

Figure 4. XRD patterns of the as-prepared precipitate and of $BaTiO_3$ samples obtained by heating the precipitate in air for 1 h. at 600−1150 °C.

crystallizes around 594 °C accompanied by the decomposition of peroxo groups. The composition of the amorphous barium peroxo-polytitanate is estimated as $BaTiO_{2.65}(O_2)_{0.35}\cdot nH_2O$ from the steep weight decrease by 2.4%.

The XRD patterns for the samples heated in air for 1 h at 600, 650, 1000, and 1150 °C are shown in Figure 4 along with that for the as-precipitated sample. The XRD patterns for the samples obtained by heating over 600 °C were coincident with those of the conventional tetragonal $BaTiO_3$ (PDF-050626), whereas the as-precipitated sample was amorphous. The crystallinity of the $BaTiO_3$ was increased from 600 to 650 °C, showing little change above 650 °C. The structural parameters for $BaTiO_3$ obtained from the Rietveld refinement are summarized in Table 1. All the XRD data were well refined with the space group *P4mm*, and showed the tetragonality ($c/a > 1$). It is important to note that $BaTiO_3$ obtained by heating at rather low temperature 600 °C also showed the tetragonality, $c/a = 1.0037$, while the low-temperature synthesis of $BaTiO_3$ in most of the earlier reports generally yielded the cubic phase. The crystallite size of $BaTiO_3$ determined from the peak profile parameters was increased almost two times from 14.7 to 25.9 nm between 600 and 650 °C. It was gradually increased from 25.9 to 48.3 nm up to

Table 1. Refined Crystallographic Data for $BaTiO_3$ Obtained by Heating the Precursor at 600−1150°C

Tetragonal; Space Group; *P4mm* (99) $Z = 1$			
atom	site	atomic position	occupancy
	600 °C, $a = 4.0148(93)$ $c = 4.0297(99)$ $c/a = 1.0037$ Crystallite Size: 14.7 nm		
Ba	1*a* (0, 0, *z*)	*z*: 0.0	0.99
Ti	1*b* (1/2,1/2, *z*)	*z*: 0.464(4)	1.0
O(1)	1*b* (1/2,1/2, *z*)	*z*: −0.068(18)	1.0
O(2)	2*c* (1/2, 0, *z*)	*z*: 0.543(23)	1.0
	650 °C, $a = 3.9998(67)$ $c = 4.0192(70)$ $c/a = 1.0049$ Crystallite Size: 25.9 nm		
Ba	1*a* (0, 0, *z*)	*z*: 0.0	0.99
Ti	1*b* (1/2,1/2, *z*)	*z*: 0.514(15)	1.0
O(1)	1*b* (1/2,1/2, *z*)	*z*: −0.058(9)	1.0
O(2)	2*c* (1/2, 0, *z*)	*z*: 0.512(85)	1.0
	1000 °C, $a = 3.9970(28)$ $c = 4.0211(28)$ $c/a = 1.0060$ Crystallite Size:48.3 nm		
Ba	1*a* (0, 0, *z*)	*z*: 0.0	0.99
Ti	1*b* (1/2,1/2, *z*)	*z*:0.493(4)	1.0
O(1)	1*b* (1/2,1/2, *z*)	*z*:-0.032(7)	1.0
O(2)	2*c* (1/2, 0, *z*)	*z*:0.519(23)	1.0
	1150 °C, $a = 3.9942(23)$ $c = 4.0302(23)$ $c/a = 1.0090$ Crystallite Size: 419.7 nm		
Ba	1*a* (0, 0, *z*)	*z*: 0.0	0.99
Ti	1*b* (1/2,1/2, *z*)	*z*: 0.526(3)	1.0
O(1)	1*b* (1/2,1/2, *z*)	*z*: 0.041(9)	1.0
O(2)	2*c* (1/2, 0, *z*)	*z*: 0.534(10)	1.0

1000 °C and sharply increased to 419.7 nm at 1150 °C. This behavior suggests that the crystal growth of $BaTiO_3$ mainly occurs by precipitation from the amorphous phase around crystal nucleus at 1000 °C or below, and that the crystal growth by fusion of fine particles proceeds around 1150 °C. The tetragonality (c/a) was increased from 1.0037 to 1.0090 with increasing temperature, suggesting that it can be controlled by changing the heating temperature. The quantitative X-ray fluorescence analysis indicated that the Ba/Ti ratios were 0.99, and thus the occupancies of Ba (1*a* site) were fixed to 0.99 in the Rietveld refinement.

The FE-SEM images of the $BaTiO_3$ samples obtained by heating the precipitate in air for 1 h at 650, 1000, and 1150 °C are shown in Figure 5a, 5b, and 5c, respectively. The $BaTiO_3$ sample obtained at 650 °C showed a uniform particle size distribution around 30 nm, and this was consistent with the crystallite size estimated from the XRD pattern. The sample obtained at 1000 °C consisted of a small number of larger particles in the range 100−200 nm and a large number of smaller particles around 50 nm. This indicates that the crystalline growth proceeds more effectively at 1000 °C than at 650 °C, and that a portion of particles fused to form larger particles partly by solid state reaction. The agglomerates of larger particles were observed in the $BaTiO_3$ sample obtained at 1150 °C. Around this temperature, the product is mostly formed through the similar process as the conventional solid state reaction, and the morphology of the product became similar to that of the conventional process.

Figure 6 shows the complex impedance plots of the pellets of $BaTiO_3$ obtained at 650, 1000, and 1150 °C.

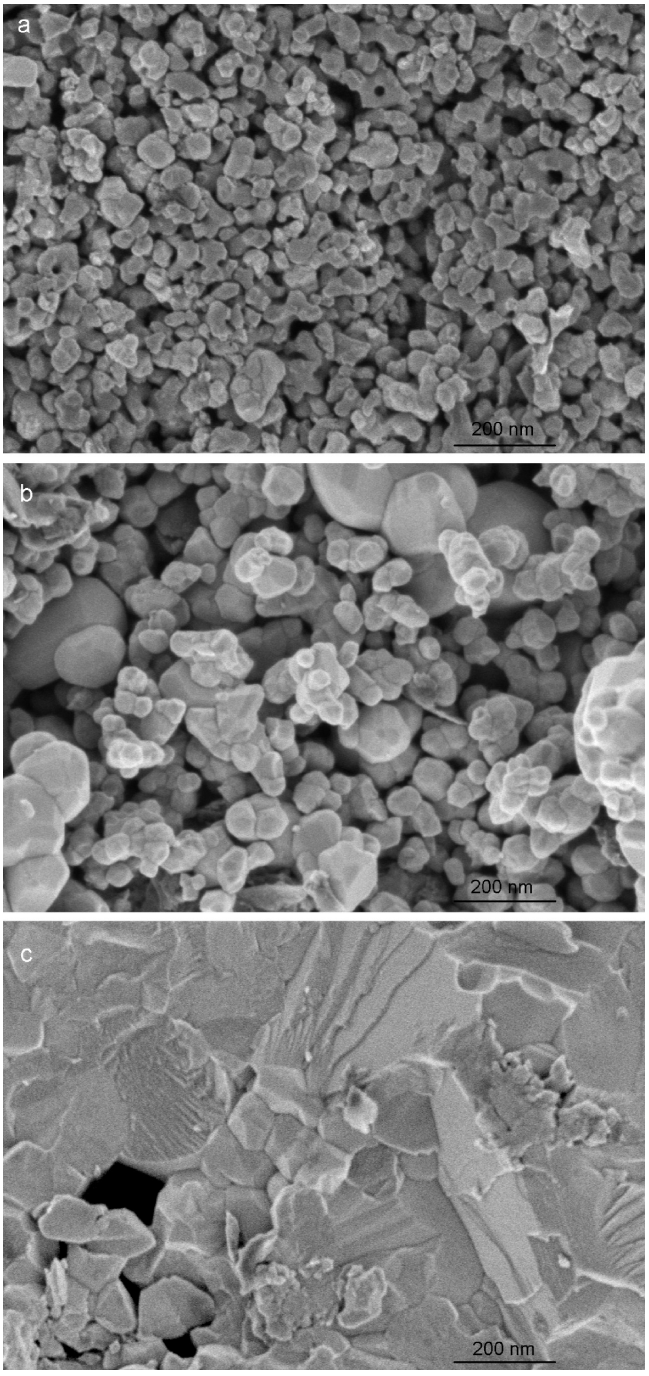

Figure 5. FE-SEM images of $BaTiO_3$ samples obtained by heating the precipitate in air for 1 h at (a) 650, (b) 1000, and (c) 1150 °C.

The dielectric constants of the pellets obtained at 650, 1000, and 1150 °C were estimated at 360, 1160, and 2990. The dielectric loss tangents of the pellets obtained at 650, 1000, and 1150 °C were 0.26, 0.30, and 0.30 at 100 kHz; and 0.08, 0.13, and 0.17 at 1 MHz, respectively. The $BaTiO_3$ particles around 25.9 nm size showed the dielectric constant of 360, and the dielectric constant increased with increasing heating temperature. The dielectric constants were closely correlated with the crystallite size and the tetragonality c/a. Our results confirmed that it is essential to maintain the tetragonality to obtain nanosized $BaTiO_3$ with high dielectric constants.

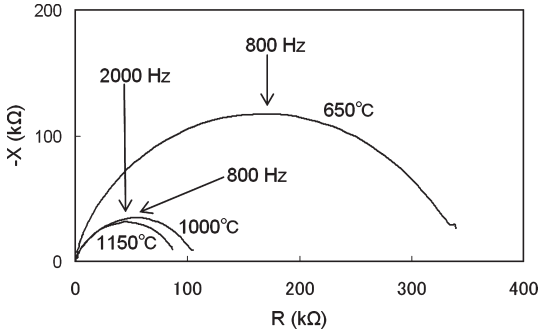

Figure 6. Complex impedance plots of the pellets of $BaTiO_3$ obtained at 650, 1000, and 1150 °C. The frequencies at the top of semicircles are indicated by arrows.

The hydrothermal syntheses in earlier reports have mostly provided cubic $BaTiO_3$ when the processing temperature was below 1000 °C[12] or the particle size was below 190 nm,[20] except for a few reports indicating tetragonal $BaTiO_3$ with $c/a = 1.0078$ prepared at 523 K[5] and with $c/a = 1.0078$, particle size of 90 nm prepared at 240 °C.[17] The oxalate decomposition methods and the sol−gel method have also provided cubic $BaTiO_3$ when the heating temperature was below 800 °C.[25,29,32] Vivekanandan and Kutty reported that the room-temperature stabilization of cubic $BaTiO_3$ prepared by the hydrothermal method was due to the presence of residual hydroxyl ions in the lattice and compensating cation vacancies.[48] They indicated that, though the hydroxyl ions were removed by heating at 900 °C, the cubic structure was retained up to 1000 °C because of the lattice strain due to the presence of the compensating cation vacancies. In contrast, by the present peroxo decomposition method, the rather high tetragonality ($c/a = 1.0037$) was achieved for the small crystallite size 14.7 nm at the preparation temperature 600 °C. This is probably because the hydroxyl ions and the cation vacancies are not involved in the amorphous peroxo-precursor. It can be said this peroxo-precursor decomposition method is appropriate to prepare nanosized $BaTiO_3$ particles with the tetragonality. Furthermore, this method can be extended to the preparation of the other titanium complex oxides such as $SrTiO_3$, $Ba_xSr_{1-x}TiO_3$, $CaTiO_3$, $Bi_{0.5}Na_{0.5}TiO_3$ by modification of the agents. We expect the peroxo-precursor will be a more commonly used precursor like the other precursors such as oxalate and citrate.

Conclusions

Ti-IPA solution was prepared by mixing metallic titanium powder and H_2O_2 aq. The preparation time of the Ti-IPA was remarkably reduced from 72 to 6 h by increasing the concentration of H_2O_2 aq from 30 to 70 wt %. $BaTiO_3$ was obtained by heating the amorphous precursor, barium peroxo-polytitanate, at 600−1150 °C, which was precipitated by mixing Ti-IPA solution with $Ba(OH)_2$ aq. The crystallite size and the tetragonality c/a were

(48) Vivekanandan, R.; Kutty, T. R. N. *Powder Technol.* **1989**, *57*, 181–192.

increased from 14.7 to 419.7 nm and from 1.0037 to 1.0090, respectively, by increasing the temperature. The crystallite size of $BaTiO_3$ obtained at 650 °C was 25.9 nm from XRD analysis, and the size distribution was homogeneous around 30 nm in the FE-SEM image. The tetragonality c/a and the dielectric constant of $BaTiO_3$ obtained at 650 °C were 1.0049 and 360, respectively. Our study demonstrates the high potential of peroxo-precursor decomposition methods for the preparation of nanosized titanium complex oxides.